Ocean and Coastal Management 262 (2025) 107573

Contents lists available at ScienceDirect

Ocean and Coastal Management

journal homepage: www.elsevier.com/locate/ocecoaman

Sensitivity of water level and flood area prediction to hurricane characteristics and climate change impacts

Ahmed Elkut [a,*], Fengyan Shi [a], Jenero Knowles [b], Casey Dietrich [b], Jack Puleo [a]

[a] Department of Civil, Construction, and Environmental Engineering, University of Delaware, Newark, DE, USA
[b] Department of Civil, Construction, and Environmental Engineering, NC State University, North Carolina, USA

A B S T R A C T

The combined impact of hurricanes and climate change can affect the total water level leading to severe impacts on coastal zones such as flooding. Accurate prediction and evaluation of water levels are essential for predicting the impact on military readiness and resilience for coastal facilities. This study uses D-Flow Flexible Mesh to evaluate the sensitivity of water level and flood area prediction to the impact of climate change and hurricane activity with application to the Naval Station Norfolk, Virginia, USA.

The water level (tide and surge) was simulated and the potential flooding resulting from historical hurricanes (Irene and Isabel) in Norfolk, VA was evaluated. The model was forced using the parametric Holland Model and various perturbations in the hurricane characteristics were evaluated. In addition, projected relative sea level rise up to the year 2150 was investigated.

D-Flow can accurately simulate the water level with an average correlation coefficient and root-mean-square-error of 0.974 and 0.17 m, respectively. Water level prediction showed high sensitivity to climate change impacts and inaccuracies in hurricane track and lower sensitivity to changes in hurricane central pressure and radius of maximum wind. A mesh resolution that reflects accurate topographical depiction is required to estimate the flood area accurately. Willoughby Spit (a narrow peninsula north of the naval base extending into Chesapeake Bay) was the most susceptible area to flooding. Significant parts of the base were found to be vulnerable to flooding under the considered scenarios, with flood areas ranging from 0.28 km2 to 5.94 km2 (1.3%–43% of the base area), with the largest predicted flooding for the sea level rise and wind speed scenarios. The insights of the sensitivity of flood predictions to various factors could enable targeted adaptation measures and resource allocation, for enhanced resilience and sustainable development in vulnerable coastal areas.

1. Introduction

Total water levels (TWL) consist of the mean sea level, tide, storm surge, and wave-induced setup and runup. Changes in the non-tidal components are highly affected by the dominant meteorological forcing (e.g. wind and atmospheric pressure), extreme weather events, and climate change.

Over 40% of the US population inhabits coastal regions (Moftakhari et al., 2015; NOAA Office for Coastal Management) and this percentage is expected to increase in the future (2023 National Population Projections). These dense population centers are at risk of severe flooding (Tang and Gallien, 2023) due to hurricanes and other storm surges (and TWL). Elevated water levels can lead to loss of human life, destruction of homes and civil infrastructure, and disruption of industry and coastal military facilities (Hanson et al., 2011; Hinkel et al., 2014; Resio and Westerink, 2008). In 2023 alone, severe storms, tropical cyclones, and flooding caused 144 deaths and cost more than $71 billion. The distribution of damage from US billion-dollar disaster events from 1980 to 2023 was dominated by tropical cyclone losses, with the highest average event cost of $22 billion (Billion-Dollar Weather and Climate Disasters | National Centers for Environmental Information (NCEI)). The North Atlantic coast of the US is particularly vulnerable to coastal flooding caused by extreme weather events such as nor'easters and hurricanes (Muis et al., 2019; Wahl et al., 2015).

Climate change-related sea level rise (SLR) is a clear risk, now and for the foreseeable future. An increase in SLR is expected to exacerbate storm-surge-related risks to coastal communities because the frequency and extent of coastal flooding are likely to increase (Vitousek et al., 2017; Ghanbari et al., 2021; Muis et al., 2023; Tanoue et al., 2016; Taherkhani et al., 2020). Relative sea level (RSL) along the contiguous US coastline is expected to rise, on average, 0.25 m–0.30 m by 2050. These estimates increase to more than 2.2 m in 2100 and 3.9 m in 2150 (relative to sea level in 2000) considering the high emission scenario (Sweet et al., 2022).

Accurate prediction of TWL for extreme events is needed to determine the potential impact on coastal zones and coastal military facility readiness and resilience (GAO, 2019; Hall et al., 2016; UOCS, 2016). These predictions will help support stakeholders and federal agencies in

* Corresponding author.
E-mail addresses: aelkut@udel.edu, corielkut@gmail.com (A. Elkut).

https://doi.org/10.1016/j.ocecoaman.2025.107573
Received 31 October 2024; Received in revised form 16 January 2025; Accepted 30 January 2025

adequate planning, prompt flood emergency response, and flood risk management decisions. Various techniques are used for coastal flood prediction including static (bathtub) and dynamic methods. The static method assumes that areas lower than a certain water level are inundated if there is hydrological connectivity. Such a technique was commonly used, in a GIS environment (Dasgupta et al., 2009; Van de Sande et al., 2012), because the physics-based sophisticated models were challenging to employ. Although computationally inexpensive (Seenath et al., 2016), the resulting flood maps often overestimate the flood extent due to the omission of important physical processes such as bottom friction, mass conservation, and flood duration (Breilh et al., 2013; Ramirez et al., 2016; Vousdoukas et al., 2016). Dynamic modeling uses sophisticated numerical models, e.g. D-Flow Flexible Mesh (FM), Advanced Circulation (ADCIRC), and the two-dimensional Hydrologic Engineering Center-River Analysis System (2D HEC-RAS) models, to simulate tides, surges, wave-induced water level, precipitation, and riverine discharges. These models have been applied successfully in coastal flood risk assessments at different scales and with varying degrees of model complexity (Bakhtyar et al., 2020; Bilskie and Hagen, 2018; Ke et al., 2019; Muñoz et al., 2022; Sebastian et al., 2014).

Most coastal flooding studies focused on the impacts of coastal water levels (often storm-surge-dominated) and fluvial or pluvial flows (Ghanbari et al., 2021; Ke et al., 2019; Kumbier et al., 2018; Nederhoff et al., 2021), or compared the performance of different hydrodynamic models in water level and flood area prediction (Bakhtyar et al., 2020; Muñoz et al., 2022). However, uncertainties and inaccuracies in model inputs (e.g. pressure drop, radius of maximum wind, and storm track) and accurate representation of the topography and bathymetry (Muñoz et al., 2020), are often understudied. Other studies evaluated the impacts of climate change on hurricanes, particularly hurricane intensity (increasing in wind speed) (Balaguru et al., 2016; Camelo et al., 2020), SLR (Balaguru et al., 2016; Mayo and Lin, 2022; Miller and Shirzaei, 2021; Pasquier et al., 2019), and rainfall (Li et al., 2022), and how they influence potential coastal flooding. However, these studies often focus on certain aspects and disregard others such as uncertainties in hurricane track and bathymetry/topography accuracy. Fossell et al. (2017) investigated the sensitivity of coastal inundation to storm tide to four hurricane parameters: track, wind speed, size, and forward speed. They evaluated the predictability of storm surge inundation affected by errors in forecasting those parameters. They disregarded the influence of SLR and the accuracy of the bathymetry/topography near the area of landfall. Liu and Huang (2020) studied the impact of hurricane tracks, wind stress, atmospheric pressure, and waves on the surge height using the ADCIRC + SWAN model around the Taiwan coast. They reported that wind stress and atmospheric pressure have a crucial role in affecting the surge height; with wave setup contributing between 6% and 35% of the storm surge. That study did not consider the associated potential flooding.

Most of the previous studies report inundation as total flood areas without classifying these areas according to the severity of the flood (flood depth) and may overlook the flood areas before and after the storm peak. Therefore, additional efforts are required to investigate the sensitivity of hurricane-induced water levels and flood prediction to climate change impacts, uncertainty in hurricane characteristics, and input data fidelity.

Building on previous work, this study investigates the prediction of water levels and associated coastal flooding under hurricane activity. The sensitivity to the impact of climate change (SLR and wind speed), perturbations in hurricane characteristics (central pressure drop, radius of maximum wind), and input data fidelity (errors in hurricane track, bathymetry/topography accuracy, and mesh resolution) were evaluated, and the nonlinear interaction between SLR and TWL were investigated. The utility of the model was evaluated according to the prediction accuracy and simulation/run time. The sensitivity of flooding was assessed based on the average and maximum flood depth, the spatial extent of flooding, and the temporal variation of these metrics. The sensitivity of peak surge prediction was evaluated against available measurements by the difference in timing, magnitude, and duration.

2. Site description

The City of Norfolk is located on the south shore of the Chesapeake Bay approximately 30 km west of the Atlantic Ocean in southeastern Virginia (USA) (Fig. 1). The city has a population of approximately 250,000 people and is home to an active military facility (Naval Station Norfolk, NSN). Norfolk includes more than 320 km of riverfront and bayfront land, including beaches along Chesapeake Bay, and is surrounded by numerous bodies of water. Norfolk and NSN are prone to flooding, much like other low-lying coastal areas, due to low elevation and proximity to natural waterways. Most of the elevation of NSN is within 5 m of mean sea level (MSL) (Li et al., 2013). The areas may face additional future strain due to high land subsidence rates (Sweet et al., 2022) and the high rate of SLR in the Chesapeake Bay, which is 2–4 times faster than the global mean SLR (Boon, 2012; Ezer et al., 2013). NSN experiences hurricane forcing and possible extratropical storm (ETS) forcing at different times of the year, making it a suitable location to test model capability under varied forcing scenarios.

The area has a mean tidal range of 0.74 m and typically experiences an east-south-easterly wind-wave climate with average significant wave heights of 0.36 m and peak periods of 5.2 s (September 2022 to November 2023, City of Norfolk, Periodic Survey Evaluation (City of Norfolk, nd). The Atlantic-fronting coastline of Willoughby Spit is characterized by average beach and surf zone (wave-breaking region) slopes of 1:30 and 1:40, respectively. In August 2011, during Hurricane Irene, Norfolk experienced significant flooding and damage on the order of $12 million. Most of the flooding occurred along Willoughby Spit with several flooded areas within NSN (STORM | System to Track, Organize, Record, and Map | Open Data Portal - City of Norfolk, VA) (STORM) Just offshore of Norfolk, the hurricane brought combined tide and surge levels of up to 1.89 m above MSL (Sewells Point), maximum wind speeds of 27.6 m/s (NDBC - Station CHLV2), and significant wave heights of up to 2.62 m (NDBC - Station 44064). During Hurricane Isabel, water levels up to 1.99 m above MSL at Sewells Point (Sewells Point – NOAA tide gauge), maximum wind speed of 33 m/s, and a significant wave height of up to 6.3 m at 25 km offshore (NDBC - Station CHLV2) were observed. Generally speaking, offshore waves approaching Chesapeake Bay dissipate or reflect at the bay entrance (Bao et al., 2015; Lin et al., 2002; BOON et al., 1996). NSN is minimally affected by waves locally generated within Chesapeake Bay, especially along the northwest boundary of the base (Sewells Point) with a wave setup of a few centimeters and negligible contribution to flooding (Li et al., 2013). Hence, wave forcing was excluded in this study and the focus is on the wind, pressure, and tide-induced water levels.

3. Approach/methods

The study was performed in three stages.

1) The water level (tide and surge) and associated flooding were simulated and the potential flooding resulting from historical hurricanes (Irene and Isabel) was evaluated at NSN. For that purpose, the D-Flow FM model (Deltares, 2023) was used. D-Flow FM has been used in complex coastal flood modeling applications (e.g., Kumbier et al., 2018; Muñoz et al., 2020; Muñoz et al., 2022; Nederhoff et al., 2021). D-Flow FM has similar water level prediction skill when compared to ADCIRC (Bakhtyar et al., 2020) and 2D HEC-RAS, (Muñoz et al., 2022). The hurricane characteristics, such as track, radius of maximum wind, central pressure, and maximum wind speed, were obtained from the National Hurricane Center (NHC).
2) The sensitivity of the modeled water level and flooding to various perturbations in the hurricane characteristics were evaluated. In

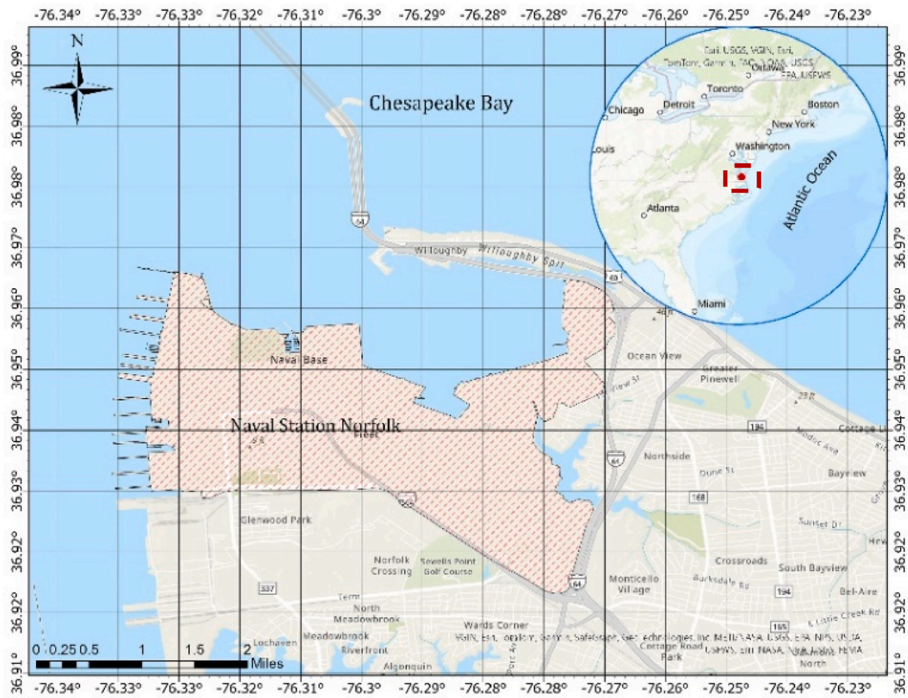

Fig. 1. Map showing Naval Station Norfolk (shaded area) with an overview map that shows the study site location (red rectangle) relative to the wider US east coast. (For interpretation of the references to color in this figure legend, the reader is referred to the Web version of this article.)

addition, the projected climate change-induced RSL, for Intermediate-Low scenarios for the US East Coast: 0.4 m, 0.8 m, 1.3 m, projected for years 2050, 2100, and 2150 (Sweet et al., 2022) respectively, were included.

3) A number of degradation scenarios were conducted to evaluate model performance when there was a deficit of accurate input data. These degradation scenarios included bathymetry error, mesh resolution, and potential error in the hurricane track.

3.1. Model setup (D-flow FM)

Delft3D FM is an open-source flexible integrated modeling suite, that simulates one-dimensional (1D), two-dimensional (2D; in either the horizontal or a vertical plane), and three-dimensional (3D) flow, sediment transport and morphology, waves, water quality, and ecology and can model the interactions between these processes. The Delft3D Flexible Mesh Suite (Delft3D FM) is the successor of the structured Delft3D 4 Suite and is developed and maintained by Deltares Netherlands as open-source software (Delft3D Flexible Mesh Suite Deltares). Delft3D FM consists of several well-tested and validated integrated modules, including D-Flow, D-Hydrology, D-Waves, and D-Morphology. D-Flow FM was used for water level, storm surge, and flood prediction in several studies along the US East Coast (Bakhtyar et al., 2020; Li et al., 2013; Muñoz et al., 2022). In this study, D-Flow FM is used to simulate the total water level combining tides and storm surges induced by hurricane winds.

3.1.1. Mesh

The computational network/mesh was created using the D-Flow FM graphical user interface (GUI) in a spherical coordinate system. The mesh has a spatial extent of 700 km in the south-north direction and an average of 480 km in the east-west direction. The mesh has rectilinear and triangular components with a resolution that decreases from 4 km at the offshore boundary to 15 m at NSN (including the base area). The mesh has about 1.5 million nodes and it was refined to have high resolution in shallower water while maintaining a reasonable computational cost.

3.1.2. Bathymetry

Numerous data sources with different resolutions and accuracies were used to represent the bathymetry and topography of the study area. These data include the continuously updated digital elevation model (CUDEM - Continuously Updated Digital Elevation Model - Bathymetric-Topographic Tiles) with a horizontal resolution of 1/9 arc-sec (~3 m) and vertical accuracy of 0.5 m and National Center for Environmental Information (NCEI) coastal relief model (CRM - (Coastal Relief Model | National Centers for Environmental Information (NCEI)) with a horizontal resolution of 1 arc-sec (~30 m) and vertical accuracy of 1 m. In addition, the general bathymetric chart for the oceans (GEBCO Gridded Bathymetry Data), with a horizontal resolution of 450 m and unknown vertical accuracy, were used for the offshore area. All data sources were combined and interpolated (Fig. 2) using the triangulation method using the D-Flow FM GUI. Higher-resolution data were used at

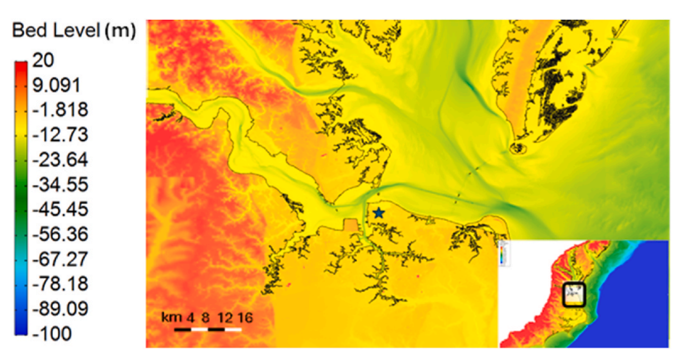

Fig. 2. D-Flow FM bathymetry/topography of NSN (MSL) with the overall model domain (inset map) of the US East Coast. Blue star shows the NSN location. The color scale is depth (m). (For interpretation of the references to color in this figure legend, the reader is referred to the Web version of this article.)

the nearshore areas, whereas lower-resolution data were used offshore.

3.1.3. Open boundary conditions

The model has three open boundaries: north, south, and east boundaries. The model was forced by two types of data along these boundaries. Tidal forces were employed as astronomical tidal components obtained from the TPXO8 global tidal model using the (Delft Dashboard - Deltares) toolbox. The solar annual and solar semi-annual were also added as tidal components.

Baroclinic changes in the water level were mimicked using the E.U. Copernicus Marine Environment Monitoring Service (CMEMS - Global Ocean Physics Analysis and Forecast | Copernicus Marine Service). Modeling baroclinic water levels requires 3D modeling that incorporates long-term baroclinic processes related to the vertical stratification of the water column, accounting for the density variations due to changes in temperature and salinity. However, in this study, only 2D depth-averaged model simulations were used. CMEMS data were referenced to the MSL to consider the baroclinic adjustment in MSL (Ye et al., 2020).

3.1.4. Meteorological forcing

Meteorological forcing was evaluated using a parameterized wind and pressure field (Holland, 1980, 2008; Holland et al., 2010). For the purpose of sensitivity tests, the wind field can be implemented easily and manipulated by changing relevant parameters such as the hurricane track, maximum wind speed (WS), radius of maximum wind (RMW), and central pressure deficit.

3.1.5. Model characteristics

The land-sea boundary was obtained from the Open Street Maps database (OpenStreetMaps) for the US East Coast. The model used a variable timestep where it computes the Courant-Friedrichs-Lewy (CFL) criterion at each timestep with an initial value of 0.7. Time steps varied from 1 to 300 s. All data were referenced to the MSL and universal coordinated time (UTC). All model simulations were run for 4 day as a spin-up period before the peak surge occurred.

4. Results

4.1. Model calibration (baseline scenarios)

Calibration for Irene was performed at different stations along the US Atlantic Coast, in Chesapeake Bay, and in the Delaware Bay (Fig. 3). Water level data were obtained at these stations from the National Oceanic and Atmospheric Administration (NOAA). Data were provided hourly and referenced to MSL. The calibration procedure was carried out for Irene and the same calibration settings were used for Isabel.

Different parameters were used during the calibration procedure of the model including the calibration of the tidal constituents (amplitude and phase). For that purpose, harmonic analysis was performed to separate the tidal water level from the non-tidal water level and the results were compared to the observed data. For the bed roughness, uniform Manning (n) bed roughness was used. Sensitivity simulations were carried out to determine the optimal Manning n value and the value of 0.023 yielded the best model performance in water level prediction, especially in capturing the peak surge. Following the 2010 Coastal Change Analysis Program (CCAP) regional land use and land cover classification data (National Oceanic and Atmospheric Administration (NOAA), 2010), it was assumed that most of the NSN base lies under the developed open space and grassland land cover categories. Both categories have a Manning n value of 0.035 (Bilskie et al., 2015). A sensitivity simulation was performed for a uniform (n: 0.023) and spatially varying Manning n value (n: 0.035 on land and 0.023 elsewhere) showed no significant differences in flood extent between both simulations. Hence, for simplicity, a uniform Manning n value of 0.023 was used for all simulations. Sensitivity to the mesh resolution was

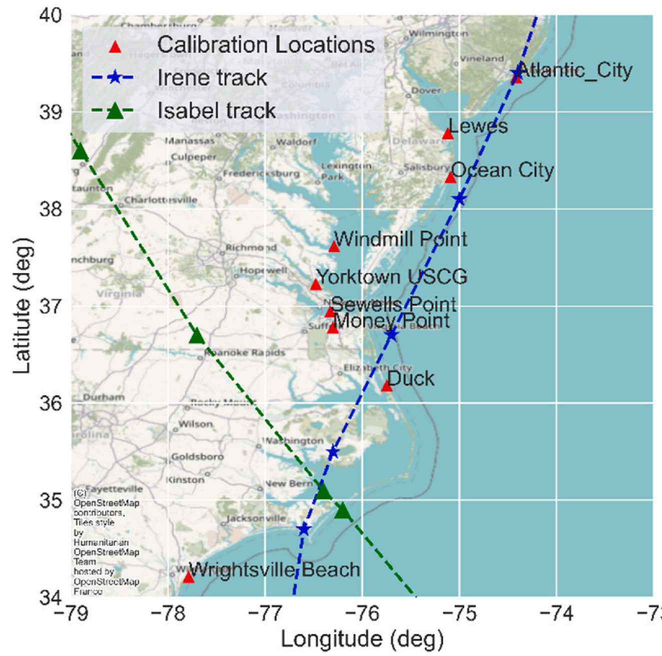

Fig. 3. Calibration locations and storm tracks for Hurricanes Irene (IR) and Isabel (IS).

evaluated and is discussed in Section 4.3.3.

Three statistics were used to quantify model skill in water level prediction:

$$\text{Correlation Coefficient}: R = \frac{\sum_{i=1}^{N}((P_i-\overline{P})(M_i-\overline{M}))}{\sqrt{\sum_{i=1}^{N}(P_i-\overline{P})^2\left(\sum_{i=1}^{N}(M_i-\overline{M})^2\right)}} \tag{1}$$

$$\text{Root Mean Square Error}: RMSE = \sqrt{\frac{1}{N}\sum_{i=1}^{N}(P_i-M_i)^2} \tag{2}$$

$$\text{Bias} = \sum_{i=1}^{N}\frac{1}{N}(P_i-M_i), \tag{3}$$

where M_i is the measured value, $\overline{M}$ is the mean value of the measured data, P_i is the predicted value, $\overline{P}$ is the mean value of the predicted data, and N is the number of data points.

Figs. 4 and 5 show an example of the comparison between the measured and simulated water levels, at Sewells Point and Duck during Irene and Isabel. Good agreement was obtained between the simulated and measured water levels. The model can capture the peak surge with high accuracy and the distributions of the measured and simulated water levels are highly comparable.

The model results show a high correlation with the measured data up to 0.99 with a root mean square error (RMSE) that ranges from 0.15 m to 0.29 m (<10% of the water level range). However, underestimations were also observed at some stations with a Bias ranging between −0.04 m and −0.2 m for both hurricanes (Table 1). These underestimations might be attributed to other factors including fluvial and pluvial impact on the water level, which were not considered in this study. In addition, although it is assumed to have a minor contribution to the TWL at NSN (Li et al., 2013), the wave-induced water level was not included in the calibration procedure. It is worth mentioning that among the nine calibration locations, some stations are located far inside the rivers discharging into the Chesapeake Bay or located close to the shoreline where bathymetry data are less accurate. Finally, unlike Irene, Isabel approached nearly perpendicular to the US east coast, approximately 200 km south of NSN. Therefore, the best model performance was

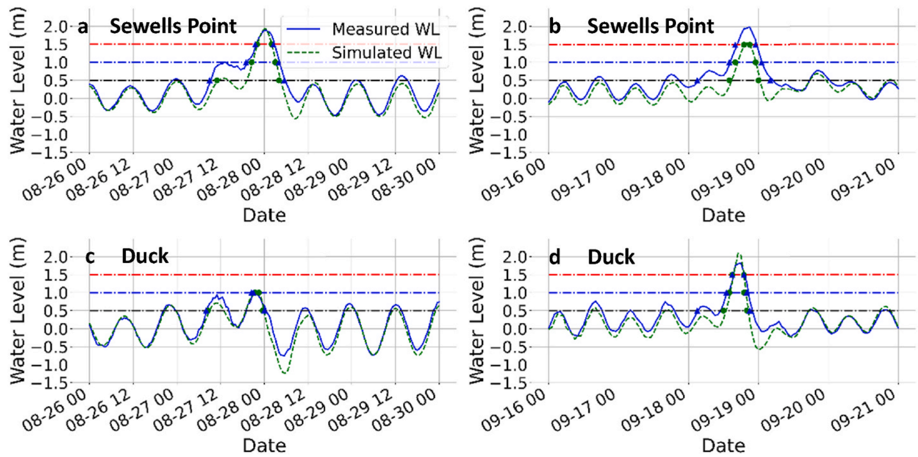

Fig. 4. Measured vs simulated water levels (MSL) showing surge duration for different surge levels during Irene (a, c) and Isabel (b, d) at Sewells Point and Duck, respectively. Dashed lines indicate high surge level (red), medium surge level (blue), and low surge level (black). (For interpretation of the references to color in this figure legend, the reader is referred to the Web version of this article.)

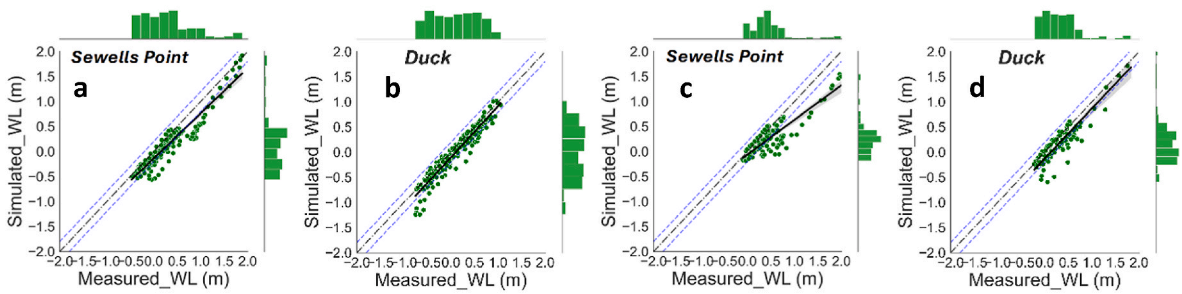

Fig. 5. Scatter plots of the measured and simulated water levels (MSL) at Sewells Point and Duck for Irene (a, b) and Isabel (c, d). Histograms are plotted along the right and upper axes.

Table 1
Summary statistics of simulated and measured water levels (MSL) at the different stations during Irene and Isabel.

#	Location	Irene			Isabel		
		R	RMSE (m)	Bias (m)	R	RMSE (m)	Bias (m)
1	Atlantic City	0.96	0.24	−0.17	0.90	0.15	−0.04
2	Lewes	0.97	0.25	−0.18	0.88	0.22	−0.13
3	Windmill Point	0.96	0.19	−0.15	0.89	0.15	−0.10
4	Yorktown	0.95	0.22	−0.15	–	–	–
5	Kiptopeke	0.97	0.16	−0.11	0.88	0.21	−0.11
6	Sewells Point	0.95	0.23	−0.17	0.88	0.29	−0.20
7	Money Point	0.94	0.27	−0.18	–	–	–
8	Duck	0.96	0.17	−0.10	0.92	0.21	−0.13
9	Wrightsville	0.96	0.20	−0.05	–	–	–

observed at Duck, NC, which is the closest station to the eye/track of Isabel. The model is robust at locations at a large distance from the hurricane eye where the impact of the hurricane itself is minor and most of the water level there is tidal driven (e.g. Atlantic City, Fig. 3).

The peak surge characteristics were evaluated based on three criteria: magnitude, duration, and timing. For peak surge magnitude and timing, a simple difference algorithm was applied to assess the model skill. For duration, the surge was classified into three levels; low: (0.5–1.0 m), medium: (1.0–1.5 m), and high: (>1.5 m). The duration of each surge level was calculated and compared to the measured data. The calculated statistics were applied to Sewells Point only due to its proximity to NSN. Good agreement was obtained between the predicted and observed water levels (Figs. 4 and 5). The model captured the peak surge during Irene at Sewells Point with a magnitude difference of 0.03 m. However, an underestimation of −0.44 m was observed during Isabel (Fig. 4). On the other hand, the timing of the peak surge was captured well by the model with almost no temporal delay. The model generally underestimates the surge duration, partially due to the underestimation in the surge magnitude. However, the maximum underestimations were −3.5 h and −15.0 h for the low-level surge for Irene and Isabel, respectively.

The severity of the flood was evaluated, as a function of the flood depth, where the flood areas were classified into four levels; low (0.1 m–0.25 m), medium (0.25 m–0.5 m), high (0.5 m–1.0 m) and extreme (>1.0 m), and a flood map was obtained for the peak flood (during the peak surge) using a shapefile that delineates the NSN area (Fig. 6b). This classification differs from the National Weather Service (NWS) coastal flood classification that comprises only three levels of flooding (minor, moderate, and major) with corresponding thresholds (0.30–0.61 m, 0.61–0.9 m, and 0.9–1.5 m) (1–2 feet, 2–3 feet, and 3–5 feet) (National Weather Service). Using the NWS classification may lead to a slight underestimation of the flood extent of 5% (compared to the predicted flood area using the adopted classification) with a flooding threshold of 0.3 m. Therefore, the four-level classification was adopted to provide a more comprehensive delineation of the flood extent.

Both hurricanes had a marginal impact on flooding of NSN where the maximum detected flood area was 0.34 km^2 and 0.24 km^2 (<2% of NSN) for Irene and Isabel, respectively. However, most of the flooded area is located at the coastal boundaries of the base where the model performance is highly affected by the large variations in the bathymetry, the accuracy of the bathymetry and topography (distinguishing wet and dry

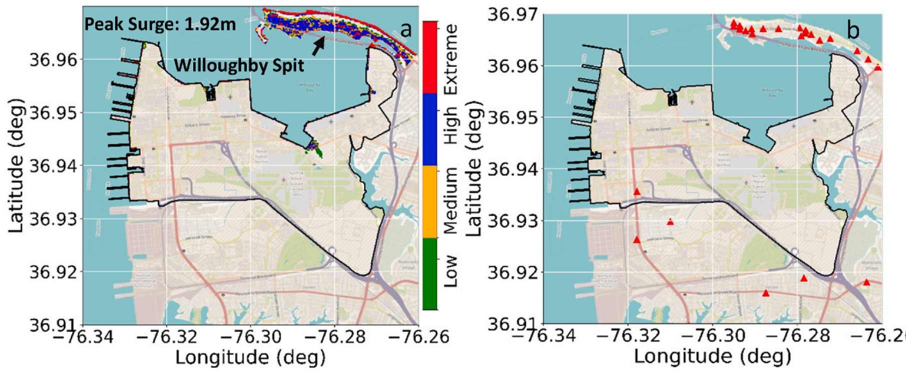

Fig. 6. Flood map with flood levels (a) and the locations of the flood areas during Irene based on the STORM anecdotal data (b). The solid black line shows the boundary of NSN, and the red triangles represent the reported flood locations. (For interpretation of the references to color in this figure legend, the reader is referred to the Web version of this article.)

cells), and the model resolution that should be high enough to capture the small changes in the water depth. The classification of the flood areas into flood levels does not reflect valuable information under this scenario because no significant flood was detected. However, for the consistency of the analysis for subsequent scenarios, flood statistics were calculated for the different flood levels (Table 2).

The final step of the calibration was to cross-reference model results to the anecdotal data obtained from the System to Track, Organize, Record, and Map (STORM) database. STORM system captures data collected by residents and city staff during and after inclement weather events. Fig. 6 shows the predicted flood areas for the entire Norfolk area (NSN and Willoughby Spit) and the locations where flood events were reported during Irene. Almost no flood locations were reported within NSN during the storm except for a single location southwest of the base, possibly attributed to pluvial flooding (heavy rain associated with the storm), which was not considered in this study. Most of the reported flooding is located at Willoughby Spit, which coincides with the model predictions. Although these data are only qualitative, they support the model results and increase confidence in the model performance at NSN. There is no additional anecdotal flood data recorded during Isabel at NSN or the surrounding area.

4.2. Impacts of meteorological forcing

Manipulating the meteorological forcing is important for understanding and evaluating the extent of influence of these forces on the severity of the hurricane impact on coastal zones. These findings may be relevant for future predictions of hurricane impacts with characteristics similar to those of the hurricanes used in this study.

4.2.1. Pressure drop (PD)

Three pressure drop (PD) scenarios were considered in this study. The central pressure deficit of each hurricane (relative to the background atmospheric pressure) was increased by 12% (PD_F0.88), 24% (PD_F0.76), and 36% (PD_F0.64) following Knutson and Tuleya (2004) and Mousavi et al. (2011). This modification resulted in minimum atmospheric pressures (PD_F0.64) of 917 mb and 887 mb for Irene and Isabel, respectively. The surge and flood area characteristics were obtained for all scenarios.

Reducing the central pressure of the hurricane caused a minor increase in the peak surge magnitude at Sewells Point of 0.03 m–0.1 m. This marginal increase in the peak surge reflected a slight increase in the surge duration with a maximum of 0.5 h. Minor changes were detected in the flood areas along NSN for all PD scenarios compared to the baseline scenarios for both hurricanes. Nevertheless, a minor increase (0.4%) in the predicted flood area was detected for Hurricane Irene due to the proximity of the hurricane eye to NSN. In addition, the average flood depth (AFD) and maximum flood depth (MFD) had a minor response under the PD_F0.64 scenario with a maximum change of 0.1 m. Otherwise, no significant impact of the PD on the flood areas was observed for both hurricanes. The other two pressure drop scenarios, PD_F0.76 and PD_F0.88 showed lower peak surge, duration, and corresponding flood areas.

4.2.2. Radius of maximum wind (RMW)

Three scenarios were considered for the RMW by reducing the radius by 10% (RMW_F0.9) and increasing it by 10% (RMW_F1.1) and 25% (RMW_F1.25) following Mousavi et al. (2011). The impact of changing the RMW was minor for both hurricanes. No significant impact was observed for the peak surge for Hurricane Irene, while a 15% increase in the peak surge was detected for Isabel for the RMW_F1.25 scenario. These minor changes in the peak surge reflect 1–2 h change in the surge duration for Isabel's high surge level. Increasing the RMW extends the area dominated by the hurricane force (increases the hurricane size), which can affect the water level before and after the peak surge. The changes in the flood areas were marginal with a maximum flood area of 3.3%. The RMW_F0.9 and RMW_F1.1 scenarios had smaller changes compared to the baseline scenarios for both hurricanes.

4.3. Impacts of climate change

4.3.1. Sea level rise

Three SLR scenarios were considered for short-term (SLR_0.4M), medium-term (SLR_0.8M), and long-term (SLR_1.3M) with 0.4 m, 0.8 m, and 1.3 m increase in the mean sea level, respectively up to 2150 following Sweet et al. (2022). Increasing the mean sea level enhanced

Table 2
Projected flood area characteristics at the peak flood during Irene and Isabel.

Flood level/Hurricane	Irene				Isabel			
	AFD (m)	MFD (m)	Flood area (km^2)	Flood %	AFD (m)	MFD (m)	Flood area (km^2)	Flood %
Low	0.18	0.25	0.01	0.11	0.17	0.25	0.01	0.07
Medium	0.37	0.5	0.02	0.17	0.37	0.49	0.01	0.10
High	0.73	1	0.04	0.3	0.77	1.00	0.03	0.23
Extreme	1.53	1.61	0.2	1.42	1.41	1.52	0.18	1.31

the peak surge magnitude and duration, which affected the potential flood areas. Including a SLR of 1.3 m increased the peak surge up to a maximum of 3.12 m (MSL) for Irene compared to 2.74 m (MSL) for Isabel (Fig. 7a). Although the nonlinearity between SLR and TWL was considered in SLR scenarios, the peak surge increased by 1.3 m ± 0.1 (SLR_1.3M) for both hurricanes. The water level increased above the medium surge level for both hurricanes for SLR_1.3M. The high surge level duration increased drastically by 13–20 h compared to 3–4.5 h for the baseline scenarios. On the other hand, the flood area (Fig. 7b) showed an increase under SLR_1.3M and SLR_0.8M scenarios with limited impact under the SLR_0.4M scenario for both hurricanes. The flood area increased from a maximum of 0.34 km^2 (<2.5%) up to 5.4 km^2 (39%) for Irene with less impacts for Isabel of 2.97 km^2 (21%) under SLR_1.3M. In addition, although the AFD showed limited change with no discernible pattern, the MFD increased up to more than 3 m (Fig. 7c).

The projected flood areas AFD, and MFD were calculated on an hourly basis for 25 h around the peak surge that occurred on August 28th at 00:00 UTC for Irene and on September 18th at 20:00 UTC for Isabel. The increase in the flood magnitude and duration, especially of the high flood level, also increased the duration of ground flooding. For instance, for Irene (Fig. 8a), the flood areas remained relatively constant below 0.5 km^2 until August 27th at 20:00 UTC, 4 h before the peak surge, when the flood area increased up to 5.4 km^2 and then started to decline again. The flood areas declined to only 2 km^2, implying these areas will be flooded for hours (maybe days) after the peak flood occurs with an AFD and MFD of 0.5 m and 2.5 m, respectively. A similar pattern was observed for Isabel but with smaller flood area of 1 km2 after hours of the hurricane passage (Fig. 8b).

The north and west parts of NSN are the most vulnerable areas to flooding with flood levels of high to extreme (>0.5 m above ground level) (Fig. 9). The extreme flood level (red color: >1 m above ground level) was concentrated at the golf course and the area adjacent to Mason Creek in the northeast part of NSN.

4.3.2. Increasing wind speed

Three scenarios for wind speed change were considered increasing the wind speed by 7.5% (WSF_1.075), 15% (WSF_1.15), and 22.5% (WSF_1.225) following Camelo et al. (2020) and Emanuel (1987).

Increasing the wind speed resulted in increasing peak surge with a maximum surge of 2.66 m and 1.82 m above mean sea level (an increase of 0.74 m and 0.27 m over the baseline) for 22.5% increase in WS for Irene and Isabel, respectively at Sewells Point (Figs. 10 and 11a). Increasing the wind speed by 7.5% showed limited impact on the surge magnitude for both hurricanes at NSN. This minimal impact is also reflected in the surge duration where there was no detection on surge levels for these two scenarios for both hurricanes. The maximum detection on surge duration was for WSF_1.225 and ranges from −0.5 h to +2.5 h for both hurricanes.

There was no change in the flood area for Isabel under this scenario group (Fig. 11b). However, the AFD and MFD increased to 1.37 m and 1.87 m, respectively. An increase in flood area was detected under the influence of Irene where 3.15 km^2 (23%) of NSN was susceptible to flooding under the WSF_1.225 scenario (Figs. 11a and 12). Most of these areas lie under the high and extreme flood categories representing 43% of the total flood area. Although the AFD decreased to 0.7 m, the MFD increased up to 2.7 m, which might have more severe consequences on the affected areas. Minor changes were also obtained for IR_WSF_1.075 and IR_WSF_1.15 scenarios with potential flood area of 4.3% and 9.3%, respectively.

The ground flood duration maintained a value of 1 km^2 (7.25%) for hours after peak surge during Irene with AFD and MFD of 0.5 m and 2.2 m, respectively. The limited increase in the flood magnitude and duration did not have an influence on the duration of ground flooding for Isabel.

4.4. Impacts of poor data resolution or availability

The lack of accurate representative data is often a challenge for modeling coastal processes. The hurricane track is one of the most important needed parameters. Inaccuracy in the track prediction can lead to underestimation of the hurricane impact at one location with overestimation at another possibly leading to loss of life or inefficient use of emergency services and evacuation orders. Bathymetric and topographic data are available from numerous sources with different resolutions and accuracies. Model domains generated from these data sources can have a significant impact on the model performance.

The performance of the model in predicting the water level and the flood areas under controlled perturbations in the hurricane track, bathymetric accuracy, and bathymetry/mesh resolution was evaluated. Six scenarios were considered for changing the hurricane track by shifting the original track to the east (STE) and the west (STW) by 54 nm, 96 nm, and 138 nm following Salehi (2018). Three scenarios were considered for bathymetric accuracy by adding Gaussian noise of 0.3 m, 0.5 m, and 1.0 m to the original bathymetry/topography data. Four scenarios were considered for changing the mesh by decreasing the resolution by factors of 5, 16, 33, and 66. These factors correspond to a maximum resolution of 75 m, 250 m, 500 m, and 1000 m, respectively.

4.4.1. Storm Track Shift (Error in Storm Track Prediction)

Irene's track was nearly coast-parallel (Fig. 3). Hence, shifting the track to the west resulted in the displacement of a significant part of the hurricane on land resulting in a lower influence on the ocean surface elevation, hence lower peak surge compared to the baseline. A large decrease in the peak surge below the low surge level (0.5 m) was predicted with the west shift of 96 nm (Figs. 13a and 14a). In addition, a negative surge down to −2 m (MSL) was predicted when shifting the track by 96 nm and 138 nm to the west where the offshore wind became the more dominant water level driving force. Shifting the hurricane track to the east (Fig. 13b) also resulted in a drop in the peak water level compared to the baseline. The influence of the hurricane becomes weaker at Sewells Point with the eye located farther offshore. The track variation results imply the original Irene track was the worst-case scenario and shifting the track to the east or to the west will result in a reduced impact on NSN. Nevertheless, the east shift scenarios have higher surge values when compared to the west shift scenarios. A similar pattern was observed for the surge duration (Table 3) where no high

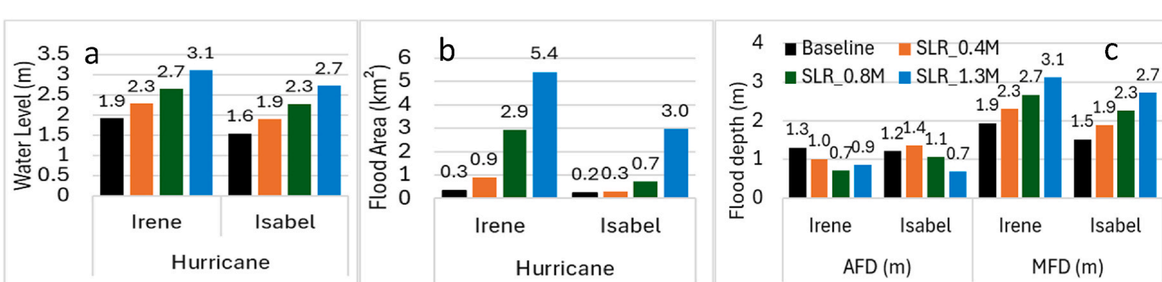

Fig. 7. Peak surge (a), flood area (b), and AFD and MFD above ground level (c) for the baseline and the SLR scenario.

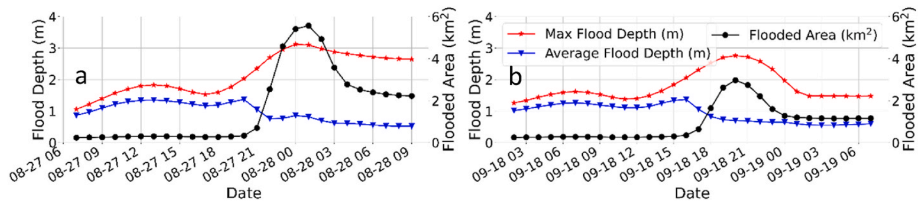

Fig. 8. Time series of the projected AFD and MFD above ground level (left axis) and flood area (right axis) for Irene (a) and Isabel (b) for SLR_1.3M scenario.

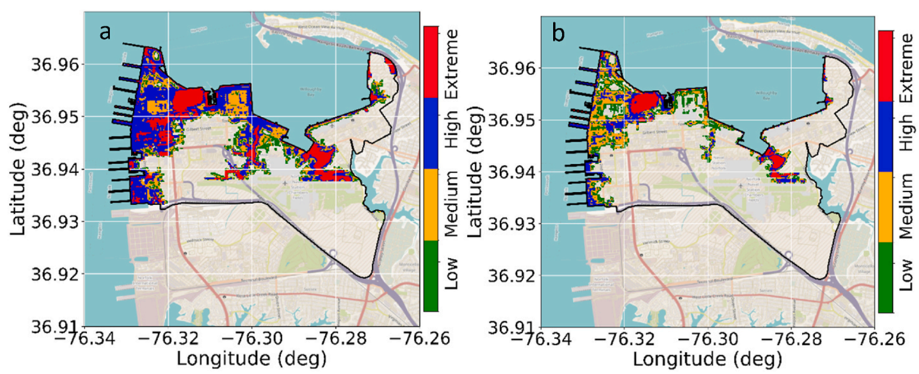

Fig. 9. Example of the flood maps with the flood levels during the peak surge for Irene (a) and Isabel (b) for the SLR_1.3M scenario.

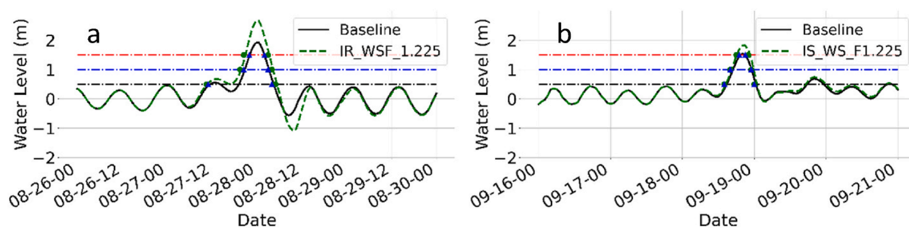

Fig. 10. Water level (MSL) time series showing the surge magnitude and duration for different surge levels for the baseline and WSF_1.225 scenarios for Irene (a) and Isabel (b) at Sewells Point. Dashed lines indicate high surge level (red), medium surge level (blue), and low surge level (black). (For interpretation of the references to color in this figure legend, the reader is referred to the Web version of this article.)

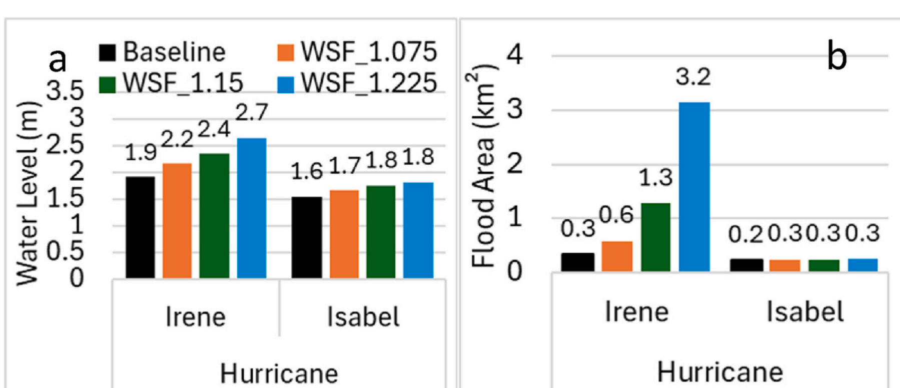

Fig. 11. Peak surge (MSL) (a) and flood areas (b) for the baseline and the WS scenario.

surge level was detected for all scenarios (zero duration). The medium surge level was detected only for the 54 nm scenarios for both shift directions but with a 30% decrease in the surge duration. The low surge level was predicted with comparable values to the baseline for the 54 nm scenarios for both shift directions. No low surge level was detected for 96 nm and 138 nm for the west shifts, while low surge duration was detected for the east shifts (96 nm and 138 nm) but with a 71% decrease in duration. The flood area statistics (Fig. 14b) showed a decrease for all simulations compared to the baseline simulation under this scenario group. The flood area decreased from 0.34 km^2 down to 0.24 km^2 (1.7%) and 0.28 km^2 (2%) for the west and east track shifts, respectively. The AFD and MFD also diminished down to 0.32 m and 0.39 m, respectively, for the west shift simulations and 0.65 m and 0.69 m, respectively, for the east shift simulations (Fig. 14c). The reduction in the flood magnitude and duration, especially of the high and medium flood levels, resulted in insignificant spatial flooding.

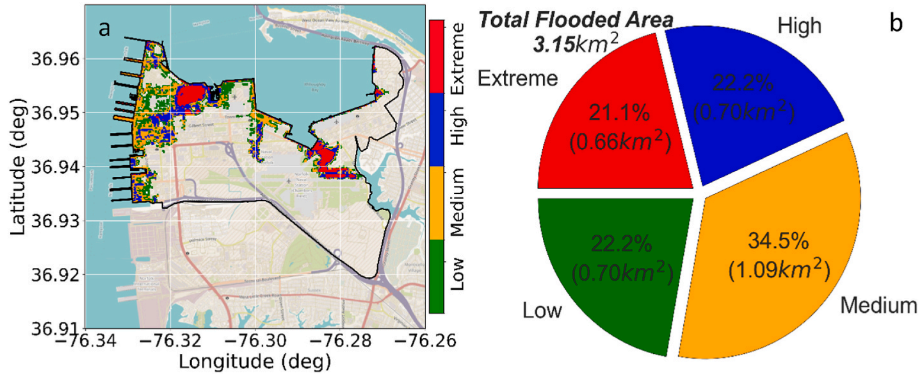

Fig. 12. Flood map with the flood levels during the peak surge (a) and the corresponding areas and percentages (b) for the WSF_1.225 scenario for Irene.

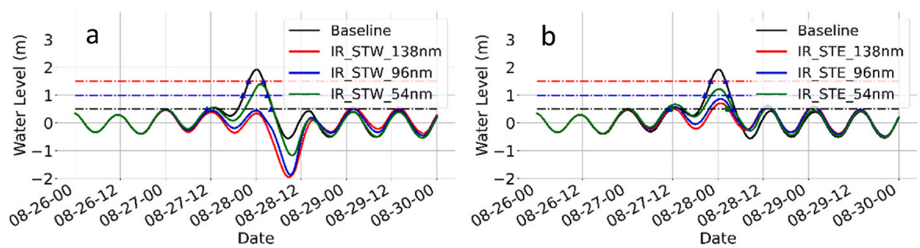

Fig. 13. Water level (MSL) time series during Irene showing the surge magnitude for different surge levels (MSL) for the baseline and storm track west shifts (a) and east shifts (b) scenarios at Sewells Point. Dashed lines indicate high surge level (red), medium surge level (blue), and low surge level (black). (For interpretation of the references to color in this figure legend, the reader is referred to the Web version of this article.)

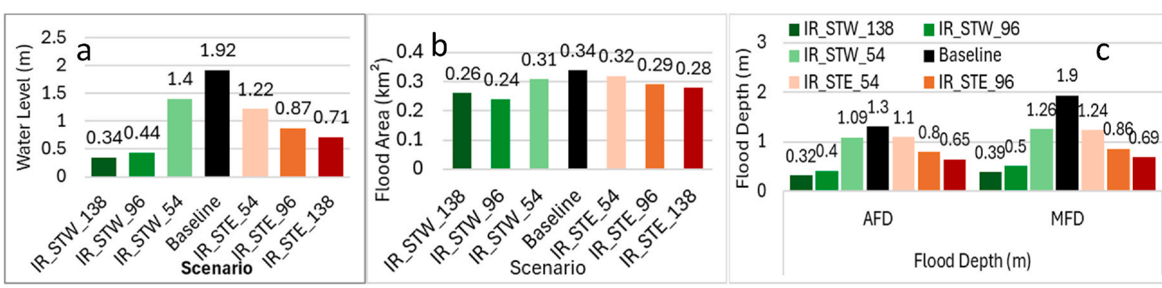

Fig. 14. Peak surge (a), flood area (b) and AFD and MFD above ground level (c) for the baseline and the storm track shift scenarios for Irene. West shifts and east shifts are in green and red gradients, respectively. (For interpretation of the references to color in this figure legend, the reader is referred to the Web version of this article.)

Table 3
Peak surge characteristics (maximum and duration) of the baseline and storm track shift scenarios for Irene at Sewells Point.

Group	Scenario	Peak Surge (m- MSL)	Duration (hours)		
			Low	Med	High
Storm Track Shift	IR_STW_138	0.34	0	0	0
	IR_STW_96	0.44	0	0	0
	IR_STW_54	1.4	18	5	0
	Baseline	1.92	17.5	7	4.5
	IR_STE_54	1.22	18.5	4.5	0
	IR_STE_96	0.87	6	0	0
	IR_STE_138	0.71	5	0	0

Isabel approached the US East coast at an angle of 325° with respect to due North where it made landfall near Drum Inlet on the Outer Banks of North Carolina (Fig. 3). Shifting Isabel to the due east or west will not have a meaningful impact on the predicted flooding. Therefore, the hurricane was shifted to the northeast (IS_STE) and to the southwest (IS_STW) at 45°.

The west shifts of Isabel resulted in a severe decrease in the peak surge down to 0.58 m (MSL) at Sewells Point with the event farther from NSN. In contrast, shifting the Isabel track to the east resulted in higher peak surge up to 3.2 m (MSL) (compared to 1.55 m for the baseline) (Fig. 15a and Table 4).This pattern is also reflected in the surge duration where an increase was detected for IS_STE_54 nm and IS_STE_96 nm scenarios up to 5 h. Shifting the track farther to the east (IS_STE_138 nm) yielded results similar to the baseline scenario. The flood characteristics (Fig. 15b) showed almost no influence of the hurricane at NSN with the west shifts and a severe impact with east shift simulations. An increase up to 6 km^2 and 5.2 km^2 was predicted for the IS_STE_54 nm and IS_STE_96 nm east shift scenarios, respectively. The AFD and MFD increased to 0.85 m and 3.25 m, respectively (Fig. 15c). This pattern was reflected on the duration of the spatial flood extent where the model predicted large flood areas (43%) with AFD and MFD of 0.5 m and 2.5 m, respectively, with the east shift simulations.

4.4.2. Bathymetry Accuracy and Resolution

Three scenarios were considered for Irene only for the effect of bathymetry accuracy by adding a Gaussian noise of 0.3 m

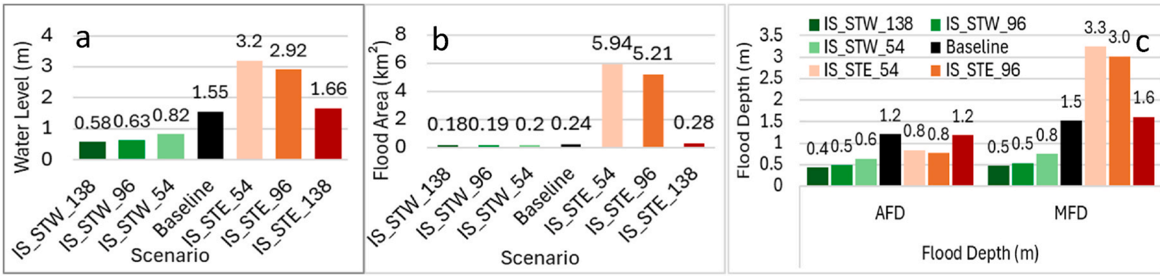

Fig. 15. Peak surge (a), Flood area (b) and AFD and MFD above ground level (c) for the baseline and the storm track shift scenarios for Isabel. West shifts and east shifts are in green and red gradients, respectively. (For interpretation of the references to color in this figure legend, the reader is referred to the Web version of this article.)

Table 4
Peak surge characteristics (maximum and duration) and flood area of the baseline and storm track shift scenarios for Isabel at Sewells Point.

Group	Scenario	Peak Surge (m-MSL)	Flood Level/Duration (hours)			FA (km^2)	FA (%)
			Low	Med	High		
Storm Track Shift	IS_STW_138	0.58	4	–	–	0.18	1.31
	IS_STW_96	0.63	5	–	–	0.19	1.38
	IS_STW_54	0.82	7	–	–	0.2	1.45
	Baseline	1.55	11	8	3	0.24	1.74
	IS_STE_54	3.2	12	10	8	5.94	43.14
	IS_STE_96	2.92	12	9	7	5.21	37.84
	IS_STE_138	1.66	9	6	3	0.28	1.31

(IR_Bathy_Acc_GN_0.3m), 0.5 m (IR_Bathy_Acc_GN_0.5m), and 1.0 m (IR_Bathy_Acc_GN_1.0m). The minor inaccuracies in the bathymetric data had no impact on the prediction of the water level and the peak surge characteristics. Although no changes were observed in the predicted peak surge magnitude and duration, an increase in the predicted flood areas was observed with a significant increase for the Bathy_Acc_GN_1.0m scenario up to 0.48 km^2 (3.5%). No detectable change was found for the AFD and MFD.

Four scenarios were considered for Irene only for the bathymetry/mesh resolution by decreasing the resolution of the baseline simulation by a factor of 5 (IR_Bathy_Res_F05), 16 (IR_Bathy_Res_F16), 33 (IR_Bathy_Res_F33), and 66 (IR_Bathy_Res_F66). The model performance in water level and peak surge prediction was still accurate even for resolution reduction down to 1000 m. A maximum change in the peak surge was −0.05 m for the Bathy_Res_F66 scenario, acceptable even with this very low-resolution mesh. However, the influence of resolution degradation on flood area prediction was substantial. The lower resolution reflected inaccurate topographic representation of NSN in terms of elevation and spatial representations. Poor resolution resulted in an unrealistic increase in the predicted flood areas for all scenarios from 0.34 km^2 (2.47%) for the baseline up to 7 km^2 (51%) for the Bathy_Res_F66 scenario. The spatial extent of the flood areas became dominated by the pixilated nature of the mesh rather than the actual topography. In addition, the AFD increased from 1.3 m for the baseline scenario up to 1.85 m. No change was found for the MFD for all scenarios.

5. Discussion

The model performance in predicting the magnitude and timing of the peak surge was accurate with an average RMSE of 0.22 m (less than 7% of the water level range) and Bias of −0.14 m. In addition, the model was able to capture the timing of the peak surge with ±1 h accuracy. These results are in good agreement with the results obtained by Bakhtyar et al. (2020). They were able to predict the TWL using D-Flow FM with a RMSE of 0.15 m–0.30 m and a Bias of −0.02 m–0.12 m during Isabel and 0.17–0.24 m and −0.14 m–0.09 m, respectively during Irene. However, they focused on Delaware Bay, and also included the fluvial effect by coupling D-Flow FM with a hydrologic model (National Water Model).

The model underestimated the water level during Isabel. Model prediction skill is highly affected by the wind input and the proximity of the area of interest to the hurricane track. Without any background wind, the Holland model (Holland, 1980) underestimates the wind field with increasing distance from the hurricane eye resulting in underestimation in the predicted water levels by up to 23% at NSN during Isabel. The model could be forced with a background wind to compensate for the underestimation. However, for areas relatively close to the hurricane track, close to the RMW, the Holland model is sufficient for the water level prediction associated with hurricane activity. Some underestimation in the duration of the different surge levels was expected due to the underestimations in the surge magnitude. However, the model generally captured the medium and high surge levels duration with acceptable accuracy (3 h within the peak surge).

Li et al. (2013) predicted the water level associated with Isabel at NSN using the Coastal Modelling System (CMS) with a RMSE of 0.076 m. Their model domain was relatively small and was forced by water level and waves from a large-scale ADCIRC simulation. They reported a 6% inundation of NSN under Isabel conditions (peak surge of 2 m-MSL). Most of the flood areas were located at the NSN golf course and Mason Creek. In the present study, because D-Flow FM underestimated the peak surge during Isabel, limited flooding was predicted. However, during Irene (peak surge 1.89 m MSL), the model predicted similar flood locations/extent at the same locations at NSN. Mason Creek is protected by a hard structure. Although including this structure might reduce any overestimation in the flood prediction (Tang and Gallien, 2023), it was not included in the model simulations due to the lack of information about its type and characteristics.

The peak surge and flood area characteristics were found to be sensitive to the climate change-related scenarios (SLR and WS scenarios) (Figs. 16 and 17). Due to low elevation at NSN, SLR will increase the water level to a point where it may result in more frequent flooding (Boon, 2012; Li et al., 2013). SLR may also result in more frequent nuisance flooding even with just high tides (Burgos et al., 2018; Moftakhari et al., 2015; Shen et al., 2022) or permanent inundation of the coastal lowland such as Willoughby Spit. To investigate the nonlinear interaction between the SLR and TWL, a 1.3 m water level offset (SLR) was added to the baseline simulation output at Sewells Point and Duck and the results were compared to the IR_SLR_1.3M scenario results at the same locations. The comparison showed minor differences between both time series revealing weak contribution of the nonlinear interaction between SLR and TWL at NSN. Moftakhari et al. (2024) studied the nonlinear interaction between the storm tide (tide + surge) and SLR at 446 sites worldwide. They showed that even with positive trend of SLR, there is a negative relationship between the SLR and the extreme water level along the US Atlantic Coast, which suggests insignificant contribution of the nonlinear interaction between the SLR and TWL in coastal

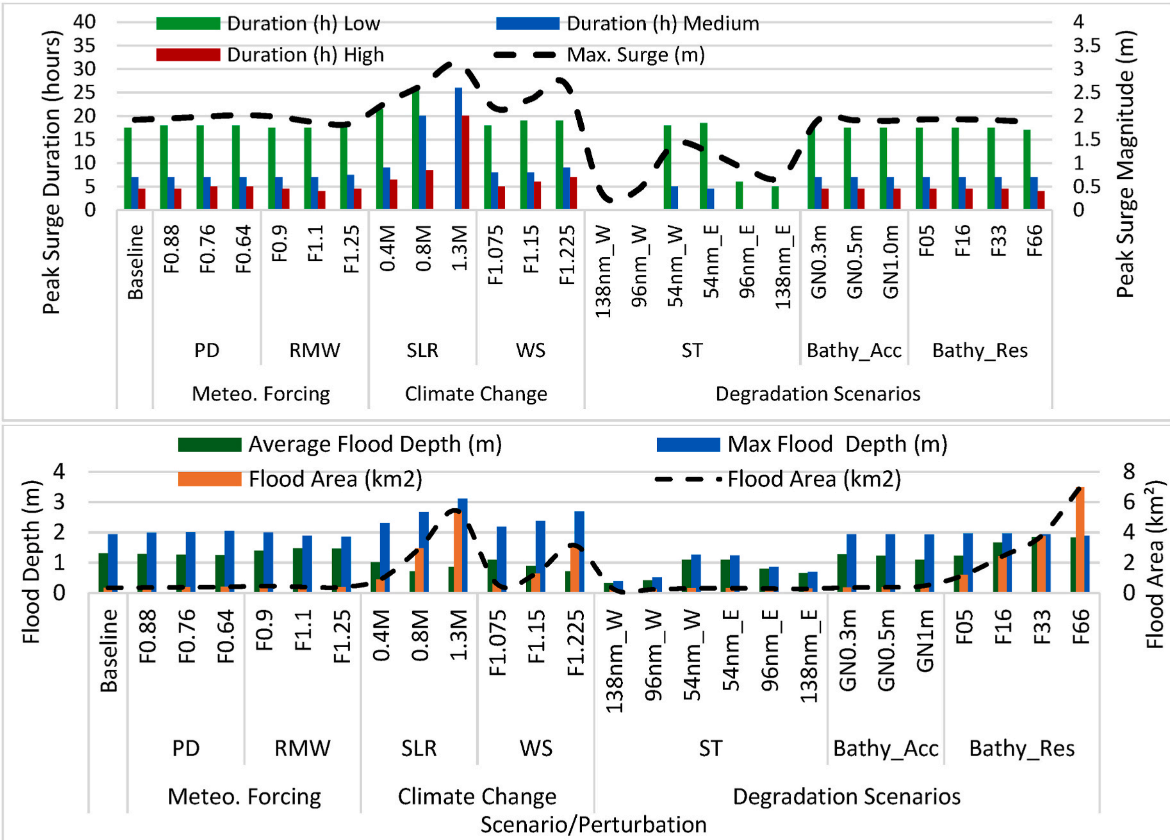

Fig. 16. Peak surge characteristics (upper panel), duration (left axis) and magnitude (right axis); and flood area statistics (lower panel), AFD and MFD (left axis) and flood area (right axis) for all scenarios for Irene.

flooding even at extreme potential SLR estimates.

The model results were sensitive to changes in the wind speed (Figs. 16 and 17) with a consistent increasing pattern in the peak surge and flood area characteristics with increasing wind speed. Increasing the wind speed by 22.5% reflected an increase in the predicted surge magnitude up to 38.5% (IR) and 17% (IS) at NSN. Isabel's storm center was more than 119 nm away from NSN with RMW of 45 nm (during the peak surge), resulting in a maximum wind speed at NSN 30%–35% lower than the maximum wind of the hurricane. Therefore, enhancing the wind speed by up to 22.5% resulted in a maximum wind at NSN lower than the maximum wind of the hurricane by 15%–20%. This deficit may explain the limited impact of the WS scenarios on the surge and flood area characteristics for Isabel at NSN. However, higher impact of enhancing the wind speed was obtained at Duck (closer to the Isabel track) with an increase in surge magnitude of 0.71 m (MSL) (46%).

The peak surge prediction showed high sensitivity to changes in the hurricane track. These changes can result in displacement of the area of interest closer to the RMW resulting in more influence on the water level, or far from the RMW, resulting in a lower water level (Bilskie et al., 2022). This effect is also dependent on the location of the area of interest to the east (onshore wind and positive surge) or the west (offshore wind and potential negative surge) of the hurricane track. This pattern is explained by the shifting of Isabel. Shifting Isabel's track to the east resulted in the displacement of the hurricane much closer to NSN causing a significant increase in the peak surge up to 3.2 m (MSL) (almost double the baseline of 1.55 m) and flood areas up to 6 km^2. Shifting the track beyond 96 nm resulted in weaker winds with a strong offshore wind direction producing a lower peak surge with low flood area characteristics that were comparable to the baseline values (Fig. 17). The offshore winds (normally on the west of the hurricane track) can produce high negative surge that can affect navigational activities rather than coastal flooding. On the other hand, Irene passed very close to NSN and, therefore with its original track, had the worst impact on NSN. Shifting the hurricane track to the east or the west resulted in a diminished impact at NSN, with probable higher impact elsewhere (Fig. 16).

The sensitivity to changes in the central pressure deficit of the hurricane (PD scenarios) was limited with the most pronounced impact on the peak surge magnitude. When increasing the central pressure deficit, the hurricane is roughly the same size, but it is more powerful near its center. This stronger hurricane had the effect of increasing the water level at the peak. D-Flow FM predicted up to a 5% increase in the peak surge above the baseline. However, the impact on surge duration and flood area was almost the same. On the other hand, changing the RMW also had a marginal impact on the surge and flood areas prediction. However, when increasing RMW, the hurricane has the same intensity, but with a much larger size. This larger hurricane had the effect of increasing the water level before and after the peak, hence increasing the surge duration (Figs. 16 and 17).

Generally speaking, model performance is proportional to the mesh resolution and the accurate representation of topography/bathymetry, especially for flood prediction simulations. However, the computational cost also increases with increasing model resolution. Therefore, a balance must be achieved between these aspects to implement feasible simulations. Degrading the bathymetry/topography accuracy and resolution showed limited influence on the model performance in terms of peak surge characteristics. The minor inaccuracies in the bathymetry/topography (up to 0.5 m) may not reflect a large change in the predicted flood area. However, an unrealistic increase (more than 50% in case of NSN) in the predicted flood area may occur when employing a very low mesh resolution (1 km) (Fig. 16). Even with a factor of 5 of resolution reduction (minimum resolution of 75 m), the predicted flood area was

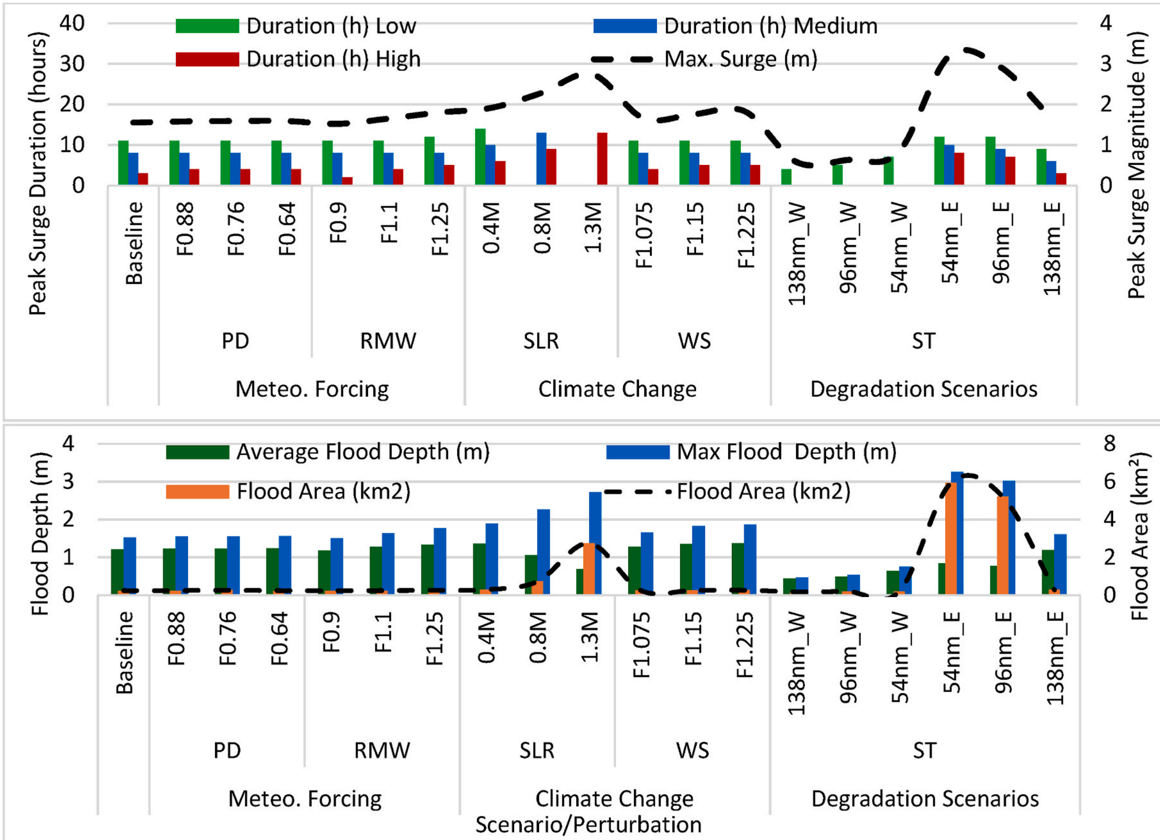

Fig. 17. Peak surge characteristics (upper panel), duration (left axis) and magnitude (right axis); and flood area statistics (lower panel), AFD and MFD (left axis) and flood area (right axis) for all scenarios for Isabel.

significantly and unrealistically higher (>8.5%) compared to the baseline. Applying more resolution reduction may result in a mesh that no longer represents the topographical nature of the area of interest. The result is a flood prediction that is driven by the pixelated nature of the mesh rather than the actual topography. However, the lower resolution reduces the computational time of model simulations. The simulation time was reduced from 14 h for the baseline simulation (15 m resolution) down to 0.35 h for the Bath_Res_F66 scenario (1 km resolution). The decision of the appropriate resolution of the model should be judged based on the main purpose of the model. For instance, if the main aim is to predict the water level and peak surge, lower-resolution fast simulations can be carried out. However, if the main purpose is to predict coastal flood areas associated with different extreme events, higher resolution, yet computationally expensive, simulations might be required. Numerous test trials should be carried out to achieve the middle ground between both approaches especially if the main aim is to develop an operational prediction model, that considers several physical and meteorological parameters, that can efficiently predict potential coastal flooding promptly to inform decision-makers.

6. Conclusions

D-Flow FM was used to evaluate the sensitivity of water level and coastal flood prediction to the combined impact of hurricanes and climate change at Norfolk, VA, USA. The model skill in water level prediction is highly dependent on the proximity of the hurricane track to the area of interest. D-Flow FM predicted the timing of the peak surge characteristics accurately. The peak surge and flood area prediction are sensitive to climate change impacts (WS and SLR). Increasing the WS by 22.5% reflects an increase in the predicted maximum surge of 17%–38.5. Increasing the sea level causes a direct influence on flood area with a maximum predicted flood area of 5.41 km^2 up to 2150 at NSN, with insignificant contribution of the nonlinear interaction between SLR and TWL. More frequent nuisance flooding is expected to occur due to SLR. Modifying the pressure drop or the radius of maximum wind has marginal impacts on the surge magnitude and flood area. However, increasing the radius of maximum wind can slightly increase the duration of the peak surge.

The results show high sensitivity to changes in the hurricane track. High surge magnitude can be obtained in the vicinity of the hurricane track with high positive or negative surge at the east or the west of the hurricane track, respectively. Potential errors in a hurricane track can lead to misleading overprediction and underprediction at incorrect locations, which can result in inaccurate decision-making. Although minor inaccuracies (up to 1 m) in the bathymetry can have limited influence on the peak surge prediction, these inaccuracies can have a significant influence on the accuracy of the flood area prediction. Reducing the mesh resolution has a high impact on flood area prediction if the mesh does not accurately represent the topography. Nonetheless, the lower resolution is also associated with lower computational cost. Therefore, choosing the appropriate model resolution depends on the main use for model output.

The findings of this work show how Holland Model wind forcing, with D-Flow FM, can be used to predict the water level under hurricane activity, with some limitations. The simulations show how the water level predictions might have relatively low sensitivity to minor changes in the pressure deficit and radius of maximum wind of the hurricane, at a specific location, and high sensitivity to the changes in the hurricane track and the climate change impacts. In addition, water level predictions can tolerate some inaccuracies in the bathymetry and mesh resolution. However, it is crucial to have an accurate representation of the wind field and the consideration of the different forces in the TWL prediction. In addition, accurate representation of the topography and coastal structures is critical for accurate flood area prediction. Finally, climate change impacts should be integrated into the long-term military infrastructure resilience plans.

The sensitivity findings of this study streamline risk assessment efforts by focusing on more impactful variables like SLR and hurricane track accuracy. They can enhance military/coastal facilities' planning and emergency response strategies. The model predictions can serve as a decision support tool for proactive coastal planning by allowing scenario simulations. For instance, the identification of flood-prone areas, like Willoughby Spit or Mason Creek, can inform the prioritization of adaptation measures at these locations and update the City of Norfolk flood zoning ordinance (City of Norfolk). This could be accomplished by revising Norfolk's flood insurance rate map (FIRM), provided by the Federal Emergency Management Agency (Federal Emergency Management Agency, 2017) (FEMA) (last updated 2017), to incorporate newly identified flood zones and their corresponding flood/risk levels.

7. Limitations

Model prediction may have suffered by ignoring the effects of river discharge and precipitation associated with the hurricanes. In addition, applying a 3D model might also be beneficial for accounting for the vertical stratification of the water column and resolving the baroclinic impact of the water that cannot be undertaken using a depth-averaged 2D model. Finally, a phase-resolving model (e.g. FUNWAVE-TVD), (Shi et al., 2012), might also be considered for incorporating the wave-induced water level components, although it is assumed to be small at the study location.

CRediT authorship contribution statement

Ahmed Elkut: Writing – review & editing, Writing – original draft, Visualization, Software, Methodology, Formal analysis, Data curation, Conceptualization. **Fengyan Shi:** Writing – review & editing, Project administration, Methodology, Conceptualization. **Jenero Knowles:** Writing – review & editing, Methodology. **Casey Dietrich:** Writing – review & editing, Methodology, Investigation. **Jack Puleo:** Writing – review & editing, Writing – original draft, Visualization, Supervision, Resources, Methodology, Funding acquisition, Conceptualization.

Declaration of competing interest

The authors declare the following financial interests/personal relationships which may be considered as potential competing interests: Ahmed Elkut reports financial support was provided by Environmental Security Technology Certification Program. If there are other authors, they declare that they have no known competing financial interests or personal relationships that could have appeared to influence the work reported in this paper.

Acknowledgements

The authors are grateful for feedback and suggestions provided by Ap van Dongeren, Kees Nederhoff, Ellen Quataert, Stephanie Patch, Jens Figlus, and Curt Storlazzi. We acknowledge funding support by the Environmental Security Technology Certification Program (ESTCP).

Data availability

Data will be made available on request.

References

2023 National Population Projections 2023 National Population Projections [WWW Document], n.d. URL https://www.census.gov/data/tables/2023/demo/popproj/2023-alternative-summary-tables.html (accessed 10.28.24).

Bakhtyar, R., Maitaria, K., Velissariou, P., Trimble, B., Mashriqui, H., Moghimi, S., Abdolali, A., Van der Westhuysen, A.J., Ma, Z., Clark, E.P., Flowers, T., 2020. A new 1D/2D coupled modeling approach for a riverine-estuarine system under storm events: application to Delaware river basin. J Geophys Res Oceans 125. https://doi.org/10.1029/2019JC015822.

Balaguru, K., Judi, D.R., Leung, L.R., 2016. Future hurricane storm surge risk for the U.S. gulf and Florida coasts based on projections of thermodynamic potential intensity. Clim. Change 138, 99–110. https://doi.org/10.1007/s10584-016-1728-8.

Bao, S., Pietrafesa, L., Yan, T., Peng, M., Gayes, P., 2015. Storm induced water levels in Norfolk Virginia and Chesapeake bay: a model and observations. Journal of Coastal Zone Management 19. https://doi.org/10.4172/2473-3350.1000415.

Billion-Dollar Weather and Climate Disasters | National Centers for Environmental Information (NCEI) [WWW Document], n.d. URL https://www.ncei.noaa.gov/access/billions/(accessed 10.28.24).

Bilskie, M.V., Hagen, S.C., 2018. Defining flood zone transitions in low-gradient coastal regions. Geophys. Res. Lett. 45, 2761–2770. https://doi.org/10.1002/2018GL077524.

Bilskie, M.V., Coggin, D., Hagen, S.C., Medeiros, S.C., 2015. Terrain-driven unstructured mesh development through semi-automatic vertical feature extraction. Adv. Water Resour. 86, 102–118. https://doi.org/10.1016/j.advwatres.2015.09.020.

Bilskie, M.V., Asher, T.G., Miller, P.W., Fleming, J.G., Hagen, S.C., Luettich, R.A., 2022. Real-time simulated storm surge predictions during Hurricane Michael (2018). Weather Forecast. 37. https://doi.org/10.1175/WAF-D-21-0132.1.

Boon, J.D., 2012. Evidence of sea level acceleration at U.S. And Canadian tide stations, atlantic coast, north America. J. Coast Res. 28, 1437–1445. https://doi.org/10.2112/JCOASTRES-D-12-00102.1.

Boon, J.D., Green, M.O., Suh, K.D., 1996. Bimodal wave spectra in lower Chesapeake Bay, sea bed energetics and sediment transport during winter storms. Cont. Shelf Res. 16 (15), 1965–1988. https://doi.org/10.1016/0278-4343(96)00011-8.

Breilh, J.F., Chaumillon, E., Bertin, X., Gravelle, M., 2013. Assessment of static flood modeling techniques: application to contrasting marshes flooded during Xynthia (western France). Nat. Hazards Earth Syst. Sci. 13, 1595–1612. https://doi.org/10.5194/nhess-13-1595-2013.

Burgos, A.G., Hamlington, B.D., Thompson, P.R., Ray, R.D., 2018. Future nuisance flooding in Norfolk, VA, from astronomical tides and annual to decadal internal climate variability. Geophys. Res. Lett. 45 (12). https://doi.org/10.1029/2018GL079572, 432-12,439.

Camelo, J., Mayo, T.L., Gutmann, E.D., 2020. Projected climate change impacts on hurricane storm surge inundation in the coastal United States. Front Built Environ 6. https://doi.org/10.3389/fbuil.2020.588049.

City of Norfolk, Periodic Survey Evaluation [WWW Document], n.d. URL https://www.norfolk.gov/Search?searchPhrase=Periodic%20Survey%20Evaluation%202023&pageNumber=1&perPage=10&departmentId=-1 (accessed 10.28.24).

City of Norfolk. (n.d.). City of Norfolk Flood Zones [WWW Document]. URL https://www.norfolk.gov/1949/Flood-Zones (accessed 1/August/2025).

Coastal Relief Model | National Centers for Environmental Information (NCEI) [WWW Document], n.d. URL https://www.ncei.noaa.gov/products/coastal-relief-model (accessed 10.28.24).

Continuously Updated Digital Elevation Model (CUDEM) - Bathymetric-Topographic Tiles [WWW Document], n.d. URL https://www.ncei.noaa.gov/access/metadata/landing-page/bin/iso?id=gov.noaa.ngdc.mgg.dem:999919 (accessed 10.28.24).

Dasgupta, S., Laplante, B., Meisner, C., Wheeler, D., Yan, J., 2009. The impact of sea level rise on developing countries: a comparative analysis. Clim. Change 93, 379–388. https://doi.org/10.1007/s10584-008-9499-5.

Delft Dashboard - Deltares [WWW Document], n.d. URL https://publicwiki.deltares.nl/display/DDB/Delft+Dashboard (accessed 10.28.24).

Delft3D Flexible Mesh Suite | Deltares [WWW Document], n.d. URL https://www.deltares.nl/en/software-and-data/products/delft3d-flexible-mesh-suite (accessed 10.28.24).

Deltares, 2023. Delft3D FM Suite Simulation Software for Safe, Sustainable and Future Deltas User Manual D-Flow Flexible Mesh.

Emanuel, K.A., 1987. The dependence of hurricane intensity on climate. Nature 326, 483–485.

Ezer, T., Atkinson, L.P., Corlett, W.B., Blanco, J.L., 2013. Gulf Stream's induced sea level rise and variability along the U.S. mid-Atlantic coast. J Geophys Res Oceans 118, 685–697. https://doi.org/10.1002/jgrc.20091.

Federal Emergency Management Agency (FEMA), 2017. Flood insurance rate map (FIRM) of Norfolk, Virginia. URL. https://orf.maps.arcgis.com/apps/StorytellingSwipe/index.html?appid=1d0754c8b069490f884d2cf1619d778e&webmap=a4adedfa962a4771aa948a661d5a8acf. (Accessed 1 August 2025).

Fossell, K.R., Ahijevych, D., Morss, R.E., Snyder, C., Davis, C., 2017. The practical predictability of storm tide from tropical cyclones in the gulf of Mexico. Mon. Weather Rev. 145, 5103–5121. https://doi.org/10.1175/MWR-D-17-0051.1.

GAO, 2019. CLIMATE RESILIENCE: DOD Needs to Assess Risk and Provide Guidance on Use of Climate Projections in Installation Master Plans and Facilities Designs (Report to Congressional Requesters No. GAO-19-453). Washington D.C.

GEBCO Gridded Bathymetry Data [WWW Document], n.d. URL https://www.gebco.net/data_and_products/gridded_bathymetry_data/(accessed 10.28.24).

Ghanbari, M., Arabi, M., Kao, S.C., Obeysekera, J., Sweet, W., 2021. Climate change and changes in compound coastal-riverine flooding hazard along the U.S. Coasts. Earth's Future 9. https://doi.org/10.1029/2021EF002055.

Global Ocean Physics Analysis and Forecast | Copernicus Marine Service [WWW Document], n.d. URL https://data.marine.copernicus.eu/product/GLOBAL_ANALYSISFORECAST_PHY_001_024/description (accessed 10.28.24).

Hall, J.A., Gill, S., Obeysekera, J., Sweet, W., Knuuti, K., Marburger, J., 2016. Regional Sea Level Scenarios for Coastal Risk Management: Managing the Uncertainty of Future Sea Level Change and Extreme Water Levels for Department of Defense Coastal Sites Worldwide.
Hanson, S., Nicholls, R., Ranger, N., Hallegatte, S., Corfee-Morlot, J., Herweijer, C., Chateau, J., 2011. A global ranking of port cities with high exposure to climate extremes. Clim. Change 104, 89–111. https://doi.org/10.1007/s10584-010-9977-4.
Hinkel, J., Lincke, D., Vafeidis, A.T., Perrette, M., Nicholls, R.J., Tol, R.S.J., Marzeion, B., Fettweis, X., Ionescu, C., Levermann, A., 2014. Coastal flood damage and adaptation costs under 21st century sea-level rise. Proc. Natl. Acad. Sci. U. S. A. 111, 3292–3297. https://doi.org/10.1073/pnas.1222469111.
Holland, G.J., 1980a. An analytic model of the wind and pressure profiles in hurricanes. Mon. Weather Rev. 108, 1212–1218. https://doi.org/10.1175/1520-0493(1980)108<1212:AAMOTW>2.0.CO, 2.
Holland, G.J., 1980b. An analytic model of the wind and pressure profiles in hurricanes. Mon. Weather Rev. 108, 1212–1218. https://doi.org/10.1175/1520-0493(1980)108<1212:AAMOTW>2.0.CO, 2.
Holland, G., 2008. A revised hurricane pressure-wind model. Mon. Weather Rev. 136, 3432–3445. https://doi.org/10.1175/2008MWR2395.1.
Holland, G.J., Belanger, J.I., Fritz, A., 2010. A revised model for radial profiles of hurricane winds. Mon. Weather Rev. 138 (1), 4393–4401. https://doi.org/10.1175/2010MWR3317.
Ke, Qian, Bricker, Jeremy, Ye, Tsinghua, 2019. Storm surge modelling by Delft3D FM – a case study in Shanghai area Ke, Qian. In: EGU General Assembly. https://doi.org/10.1023/A:1015876701363. Vienna.
Knutson, T.R., Tuleya, R.E., 2004. Impact of CO 2-induced warming on simulated hurricane intensity and precipitation: sensitivity to the choice of climate model and convective parameterization. J. Clim. 17, 3477–3495.
Kumbier, K., Carvalho, R.C., Vafeidis, A.T., Woodroffe, C.D., 2018a. Investigating compound flooding in an estuary using hydrodynamic modelling: a case study from the Shoalhaven River, Australia. Nat. Hazards Earth Syst. Sci. 18, 463–477. https://doi.org/10.5194/nhess-18-463-2018.
Kumbier, K., Carvalho, R.C., Vafeidis, A.T., Woodroffe, C.D., 2018b. Investigating compound flooding in an estuary using hydrodynamic modelling: a case study from the Shoalhaven River, Australia. Nat. Hazards Earth Syst. Sci. 18, 463–477. https://doi.org/10.5194/nhess-18-463-2018.
Li, H., Lin, L., Burks-Copes, K.A., 2013. Modeling of coastal inundation, storm surge, and relative sea-level rise at Naval Station Norfolk, Norfolk, Virginia, U.S.A. J. Coast Res. 29, 18–30. https://doi.org/10.2112/JCOASTRES-D-12-00056.1.
Li, X., Fu, D., Nielsen-Gammon, J., Gangrade, S., Kao, S.-C., Chang, P., Morales Hernández, M., Voisin, N., Zhang, Z., Gao, H., 2022. Impacts of climate change on future hurricane induced rainfall and flooding in a coastal watershed. A Case Study on Hurricane Harvey.
Lin, W., Sanford, L.P., Suttles, S.E., 2002. Wave measurement and modeling in Chesapeake Bay. Cont. Shelf Res. 22, 2673–2686. https://doi.org/10.1016/S0278-4343(02)00120-6.
Liu, W.C., Huang, W.C., 2020. Investigating typhoon-induced storm surge and waves in the coast of Taiwan using an integrally-coupled tide-surge-wave model. Ocean Eng. 212. https://doi.org/10.1016/j.oceaneng.2020.107571.
Mayo, T.L., Lin, N., 2022. Climate change impacts to the coastal flood hazard in the northeastern United States. Weather Clim. Extrem. 36. https://doi.org/10.1016/j.wace.2022.100453.
Miller, M.M., Shirzaei, M., 2021. Assessment of Future Flood Hazards for Southeastern Texas: Synthesizing Subsidence, Sea-Level Rise, and Storm Surge Scenarios. Geophys. Res. Lett. 48. https://doi.org/10.1029/2021GL092544.
Moftakhari, H.R., AghaKouchak, A., Sanders, B.F., Feldman, D.L., Sweet, W., Matthew, R. A., Luke, A., 2015. Increased nuisance flooding along the coasts of the United States due to sea level rise: Past and future. Geophys. Res. Lett. 42, 9846–9852. https://doi.org/10.1002/2015GL066072.
Moftakhari, H., Muñoz, D.F., Akbari Asanjan, A., AghaKouchak, A., Moradkhani, H., Jay, D.A., 2024. Nonlinear Interactions of Sea-Level Rise and Storm Tide Alter Extreme Coastal Water Levels: How and Why? AGU Advances 5. https://doi.org/10.1029/2023AV000996.
Mousavi, M.E., Irish, J.L., Frey, A.E., Olivera, F., Edge, B.L., 2011. Global warming and hurricanes: The potential impact of hurricane intensification and sea level rise on coastal flooding. Clim. Change 104, 575–597. https://doi.org/10.1007/s10584-009-9790-0.
Muis, S., Lin, N., Verlaan, M., Winsemius, H.C., Ward, P.J., Aerts, J.C.J.H., 2019. Spatiotemporal patterns of extreme sea levels along the western North-Atlantic coasts. Sci. Rep. 9. https://doi.org/10.1038/s41598-019-40157-w.
Muñoz, D.F., Moftakhari, H., Moradkhani, H., 2020a. Compound Effects of Flood Drivers and Wetland Elevation Correction on Coastal Flood Hazard Assessment. Water Resour. Res. 56. https://doi.org/10.1029/2020WR027544.
Muñoz, D.F., Moftakhari, H., Moradkhani, H., 2020b. Compound Effects of Flood Drivers and Wetland Elevation Correction on Coastal Flood Hazard Assessment. Water Resour. Res. 56. https://doi.org/10.1029/2020WR027544.
Muñoz, D.F., Yin, D., Bakhtyar, R., Moftakhari, H., Xue, Z., Mandli, K., Ferreira, C., 2022a. Inter-Model Comparison of Delft3D-FM and 2D HEC-RAS for Total Water Level Prediction in Coastal to Inland Transition Zones. J. Am. Water Resour. Assoc. 58, 34–49. https://doi.org/10.1111/1752-1688.12952.
Muñoz, D.F., Yin, D., Bakhtyar, R., Moftakhari, H., Xue, Z., Mandli, K., Ferreira, C., 2022b. Inter-Model Comparison of Delft3D-FM and 2D HEC-RAS for Total Water Level Prediction in Coastal to Inland Transition Zones. J. Am. Water Resour. Assoc. 58, 34–49. https://doi.org/10.1111/1752-1688.12952.
National Oceanic and Atmospheric Administration (NOAA), 2010. Coastal Change Analysis Program (C-CAP). Regional Land Cover Classification Scheme.
National Weather Service (NWS). (n.d.). Coastal Flooding Thresholds. URL https://www.weather.gov/media/erh/erhcoast/CoastalFloodThresholds.pdf.
NDBC - Station 44064 - First Landing, VA [WWW Document], n.d. URL https://www.ndbc.noaa.gov/station_history.php?station=44064 (accessed 10.28.24).
NDBC - Station CHLV2 [WWW Document], n.d. URL https://www.ndbc.noaa.gov/station_page.php?station=CHLV2 (accessed 10.28.24).
Nederhoff, K., Saleh, R., Tehranirad, B., Herdman, L., Erikson, L., Barnard, P.L., van der Wegen, M., 2021a. Drivers of extreme water levels in a large, urban, high-energy coastal estuary – A case study of the San Francisco Bay. Coast. Eng. 170. https://doi.org/10.1016/j.coastaleng.2021.103984.
Nederhoff, K., Saleh, R., Tehranirad, B., Herdman, L., Erikson, L., Barnard, P.L., van der Wegen, M., 2021b. Drivers of extreme water levels in a large, urban, high-energy coastal estuary – A case study of the San Francisco Bay. Coast. Eng. 170. https://doi.org/10.1016/j.coastaleng.2021.103984.
NOAA Office for Coastal Management, Economics and Demographics [WWW Document], n.d. URL https://coast.noaa.gov/states/fast-facts/economics-and-demographics.html (accessed 10.28.24).
OpenStreetMaps [WWW Document], n.d. URL https://osmdata.openstreetmap.de/data/land-polygons.html (accessed 10.28.24).
Pasquier, U., He, Y., Hooton, S., Goulden, M., Hiscock, K.M., 2019. An integrated 1D–2D hydraulic modelling approach to assess the sensitivity of a coastal region to compound flooding hazard under climate change. Nat. Hazards 98, 915–937. https://doi.org/10.1007/s11069-018-3462-1.
Ramirez, J.A., Lichter, M., Coulthard, T.J., Skinner, C., 2016. Hyper-resolution mapping of regional storm surge and tide flooding: comparison of static and dynamic models. Nat. Hazards 82, 571–590. https://doi.org/10.1007/s11069-016-2198-z.
Resio, D.T., Westerink, J.J., 2008. Modeling the physics of storm surges. Phys. Today 61, 33–38. https://doi.org/10.1063/1.2982120.
Salehi, M., 2018. Storm surge and wave impact of low-probability hurricanes on the lower Delaware Bay-Calibration and application. J. Mar. Sci. Eng. 6, 1–28. https://doi.org/10.3390/jmse6020054.
Sebastian, A., Proft, J., Dietrich, J.C., Du, W., Bedient, P.B., Dawson, C.N., 2014. Characterizing hurricane storm surge behavior in Galveston Bay using the SWAN+ADCIRC model. Coast. Eng. 88, 171–181. https://doi.org/10.1016/j.coastaleng.2014.03.002.
Seenath, A., Wilson, M., Miller, K., 2016. Hydrodynamic versus GIS modelling for coastal flood vulnerability assessment: Which is better for guiding coastal management? Ocean Coast Manag. 120, 99–109. https://doi.org/10.1016/j.ocecoaman.2015.11.019.
Sewells Point – NOAA tide gauge [WWW Document], n.d. URL https://tidesandcurrents.noaa.gov/waterlevels.html?id=8638610&bdate=20240101&edate=20240201&units=metric&timezone=GMT&interval=6 (accessed 10.28.24).
Shen, Y., Tahvildari, N., Morsy, M.M., Huxley, C., Chen, T.D., Goodall, J.L., 2022. Dynamic Modeling of Inland Flooding and Storm Surge on Coastal Cities under Climate Change Scenarios: Transportation Infrastructure Impacts in Norfolk, Virginia USA as a Case Study. Geosciences 12. https://doi.org/10.3390/geosciences12060224.
Shi, F., Kirby, J.T., Harris, J.C., Geiman, J.D., Grilli, S.T., 2012. A high-order adaptive time-stepping TVD solver for Boussinesq modeling of breaking waves and coastal inundation. Ocean Model. 43–44, 36–51. https://doi.org/10.1016/j.ocemod.2011.12.004.
STORM | System to Track, Organize, Record, and Map | Open Data Portal - City of Norfolk, VA [WWW Document], n.d. URL https://data.norfolk.gov/Public-Safety/STORM-System-to-Track-Organize-Record-and-Map/mrv3-rcpc/about_data (accessed 10.28.24).
Sweet, W.V., Hamlington, B.D., Kopp, R.E., Weaver, C.P., Barnard, P.L., Bekaert, D., Brooks, W., Craghan, M., Dusek, G., Frederikse, T., Garner, G., Genz, A.S., Krasting, J.P., Larour, E., Marcy, D., Marra, J.J., Obeysekera, J., Osler, M., Pendleton, M., Roman, D., Schmied, L., Veatch, W., White, K.D., Zuzak, C., 2022. Global and Regional Sea Level Rise Scenarios for the United States.
Tang, B., Gallien, T.W., 2023. Predicting Compound Coastal Flooding in Embayment-Backed Urban Catchments: Seawall and Storm Drain Implications. J. Mar. Sci. Eng. 11. https://doi.org/10.3390/jmse11071454.
UOCS, 2016. The US Military on the Front Lines of Rising Seas (EXECUTIVE SUMMARY).
Van de Sande, B., Lansen, J., Hoyng, C., 2012. Sensitivity of coastal flood risk assessments to digital elevation models. Water (Switzerland) 4, 568–579. https://doi.org/10.3390/w4030568.
Vitousek, S., Barnard, P.L., Fletcher, C.H., Frazer, N., Erikson, L., Storlazzi, C.D., 2017. Doubling of coastal flooding frequency within decades due to sea-level rise. Sci. Rep. 7. https://doi.org/10.1038/s41598-017-01362-7.
Vousdoukas, M.I., Voukouvalas, E., Mentaschi, L., Dottori, F., Giardino, A., Bouziotas, D., Bianchi, A., Salamon, P., Feyen, L., 2016. Developments in large-scale coastal flood hazard mapping. Nat. Hazards Earth Syst. Sci. 16, 1841–1853. https://doi.org/10.5194/nhess-16-1841-2016.
Wahl, T., Jain, S., Bender, J., Meyers, S.D., Luther, M.E., 2015. Increasing risk of compound flooding from storm surge and rainfall for major US cities. Nat. Clim. Change 5, 1093–1097. https://doi.org/10.1038/nclimate2736.
Ye, F., Zhang, Y.J., Yu, H., Sun, W., Moghimi, S., Myers, E., Nunez, K., Zhang, R., Wang, H.V., Roland, A., Martins, K., Bertin, X., Du, J., Liu, Z., 2020. Simulating storm surge and compound flooding events with a creek-to-ocean model: Importance of baroclinic effects. Ocean Model. 145. https://doi.org/10.1016/j.ocemod.2019.101526.